Optica Applicata, Vol. XLVI, No. 4, 2016
DOI: 10.5277/oa160405

Mode conversion in two-dimensional magneto-photonic crystal waveguide made by fully compatible optical sol-gel matrix

AHMED KAHLOUCHE*, ABDESSELAM HOCINI, DJAMEL KHEDROUCHE

Laboratoire d'Analyse des Signaux et Systèmes (LASS), Département d'Electronique,
Faculté de Technologie, Université Mohamed Boudiaf de M'sila,
BP.166, Route Ichebilia, M'sila 28000, Algeria

*Corresponding author: kahlouche_ahmed@yahoo.fr

In this paper, we have reported a theoretical study of the mode conversion in two-dimensional magneto-photonic crystal waveguide. The structure is formed by a triangular lattice of air holes embedded in a composite matrix SiO_2/ZrO_2 or SiO_2/TiO_2. These new magneto-optical materials are developed by organic-inorganic sol-gel process and doped with ferrite of cobalt nanoparticles ($CoFe_2O_4$). The modal birefringence and conversion output have been calculated by varying, respectively, the film thickness and the magnetic nanoparticles concentration. The obtained results show an enhancement in the TE-TM mode conversion. Thus, when the amount of cobalt ferrite nanoparticles reaches 39% into sol-gel matrix, the efficiency can reach 95% which proves that such structures have very promising potential for creating integrated optical isolators.

Keywords: magneto-photonic crystal waveguides, modal birefringence, optical isolator, mode conversion TE-TM.

1. Introduction

Magneto-optical isolators are the essential nonreciprocal devices which are used in optical communication systems. These components are based on the Faraday rotation effect of magneto-optical materials and its nonreciprocal behavior [1, 2]. Optical isolators allow the transmission of light in only one direction and block it in the opposite direction. Because of this performance, the optical isolator is necessary for protecting other optical active devices such as an amplifier and laser source from unwanted reflections [3, 4].

Nowadays, there is a strong interest in the miniaturization of nonreciprocal devices in order to integrate all optical components on a unique substrate. Several years ago, the material widely used to fabricate bulk optical isolators is the ferrimagnetic garnet oxide crystal yttrium iron garnet (YIG), or bismuth substituted yttrium iron garnet (Bi:YIG) deposited on a gadolinium gallium garnet (GGG) substrate [5]. However, this class of

material cannot be easily embedded by classical technologies to realize magneto-optical integrated devices because the annealing temperature needed for the crystallization of magnetic Iron Garnet which is as high as 700°C [6]. In the other hand, the use of GGG as a substrate is not commonly used to realize integrated functions based on III-V semiconductor, silica, silicon and polymer [7]. To overcome these problems, several groups of research have developed a novel approach based on a composite magneto-optical matrix doped with magnetic nanoparticles [8, 9]. Sol-gel process can be used to prepare a large variety of thin films obtained on several substrates (glass, silicon) and fully compatible with planar magneto-photonic crystal waveguides [10, 11].

The magneto-optical materials made by SiO_2/ZrO_2 or SiO_2/TiO_2 matrix doped with 1.5% of cobalt ferrite ($CoFe_2O_4$) present an interest Faraday rotation about 320 deg/cm at 1.55 μm, but it is suffering from a low merit factor, which is the quality ratio between the Faraday rotation and the absorption ($F = \theta_F/\alpha$ [deg·cm^{-1}/cm^{-1}]), it is about 12 deg at 1.55 μm for planar waveguides [12]. However, this value of a merit factor is motivating, but is not enough to consider this magneto-optical material as a good candidate for integrated applications.

Based on our previous paper [13], we present in this paper a new structure called 2D magneto-photonic crystal waveguides which are used for amplifying the magneto -optical effects in order to enhance the merit factor. Using a beam propagation method (BPM) [14], we look to investigate the influence of the volume fraction of magnetic nanoparticles and the film thickness on the mode conversion in 2D magneto-photonic waveguides formed with a triangular lattice of circular air holes.

2. Two-dimensional photonic crystal

The two-dimensional photonic crystal to be studied and analyzed in this work is shown in Fig. 1**a**. The structure consists of a triangular lattice of circular air holes embedded in a SiO_2/ZrO_2 or SiO_2/TiO_2 organic-inorganic matrix. The air holes have a radius of $0.36a$, where a is the lattice constant (a = 750 nm). However, the triangular lattice al-

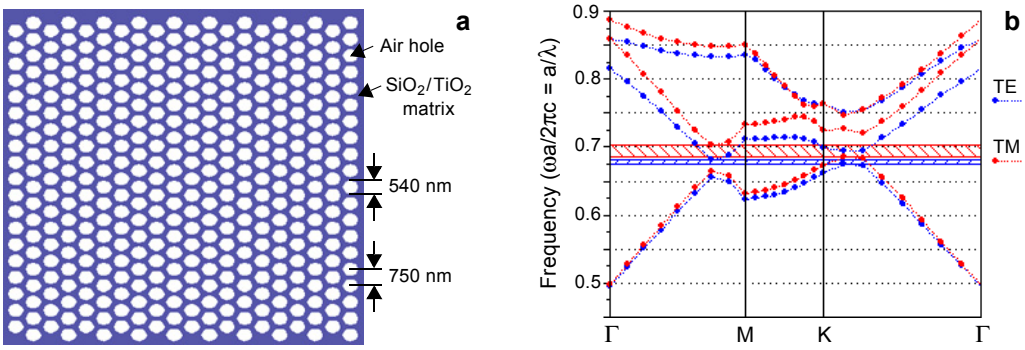

Fig. 1. The 2D photonic crystal structure formed by a triangular lattice of air holes in a composite matrix (**a**), and TE/TM band structure for a 2D photonic crystal formed by a triangular lattice of circular air holes in a composite matrix SiO_2/TiO_2 (**b**).

T a b l e 1. Refractive index of the host matrix at 1.55 μm [17].

Ratio SiO_2/ZrO_2 or TiO_2	Precursors	Index at 1.55 μm
Sol 10/3	SiO_2, ZrO_2	1.504
Sol 10/7	SiO_2, ZrO_2	1.515
Sol 10/10	SiO_2, ZrO_2	1.528
Sol 10/12	SiO_2, TiO_2	1.580
Sol 10/10	SiO_2, TiO_2	1.575

lows the opening of 2D photonic band gap, presents a good compromise, namely for high felling factors, and it is lowly sensitive to the incidence angle compared to the square lattice [15, 16]. Moreover, the triangular lattice is expected to serve a good platform for photonic integrated circuits. The composite matrix is prepared by sol-gel process and is characterized by a weak and a flexible index which can be changed in the range 1.51 to 1.58 at the wavelength of telecommunications $\lambda = 1.55$ μm, as mentioned in Table 1 [17].

The 2D photonic crystal is characterized by a low refractive index ($n = 1.58$) [17]. Different results (obtained by using a 2D plane wave expansion (PWE) method) present simultaneously the photonic band gaps formed for both polarizations: transverse magnetic (TM) and transverse electric (TE). Figure 1**b** sketches the dispersions curves and band gaps which are calculated along the Γ–M–K–Γ edge for the Brillouin zone of the structure without any defects, for both polarizations (TM and TE). On the one hand, we see that the largest band gap opened is for the TM polarization which is indicated by the hashed red region, it extends from normalized frequency $a/\lambda = 0.468$ to 0.505 whose corresponding wavelength ranges from $\lambda = 1.485$ μm to 1.602 μm. On the other hand, a narrow band gap will appear for the TE polarization, it extends from $a/\lambda = 0.447$ to 0.461 whose corresponding wavelength spans from $\lambda = 1.626$ μm to 1.677 μm.

Figures 2**a** and 2**b** show respectively the influence of a slab index on the size and position of the photonic band gaps for 2D photonic crystal described above. From

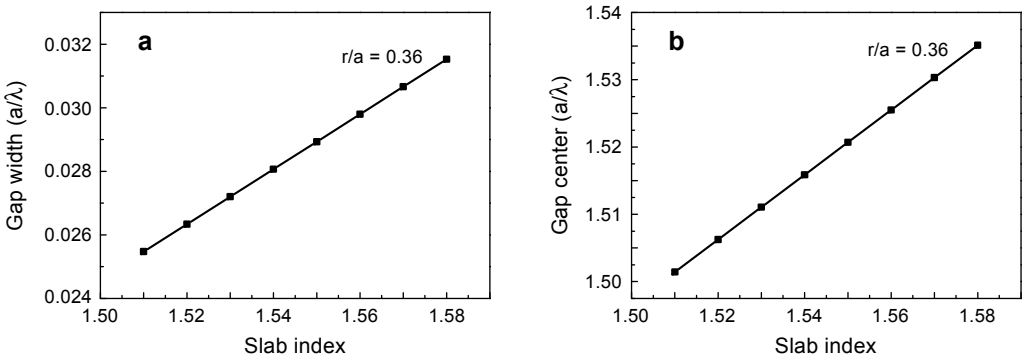

Fig. 2. Variation of the TM photonic band gap width (**a**), and variation of the wavelength center of TM photonic band gap (**b**) as a function of slab index for $r/a = 0.36$.

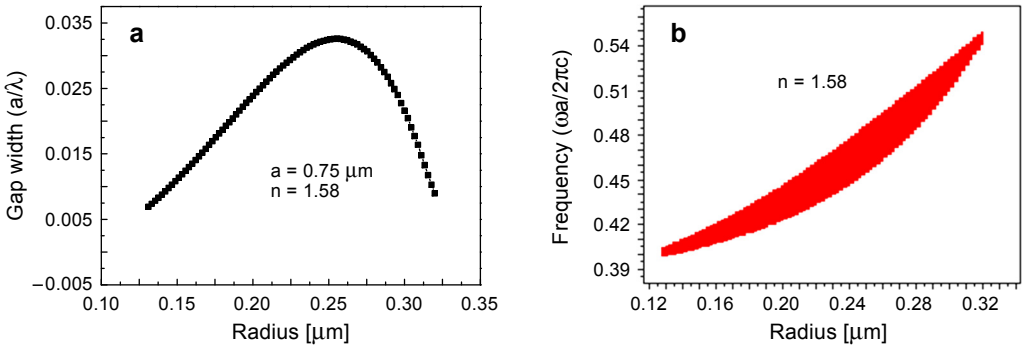

Fig. 3. Band gap width as a function of air hole radius of a 2D photonic crystals (**a**). Gap map of 2D photonic crystals structure formed by a triangular lattice of circular air holes insert in sol-gel SiO_2/TiO_2 matrix (**b**).

results, we can conclude that the width of photonic band gaps is strongly influenced by the refractive index. The band width in normalized frequency was increased from $\Delta(a/\lambda) = 0.02547$ for low index ($n = 1.51$) to $\Delta(a/\lambda) = 0.03153$ for high index ($n = 1.58$). On the other hand, the results demonstrate clearly that when the refractive index increases, the photonic band gap shifts towards the higher wavelengths, and the center wavelength $\lambda_c = (\lambda_{min} + \lambda_{max})/2$ varied from $\lambda_c = 1.501$ μm to 1.535 μm.

In Figure 3**a**, we have reported the variations of the bandwidth as a function of air hole radius for a lattice period $a = 0.75$ μm and a refractive index equal to 1.58. The results show that the band gaps were opened from $r = 0.131$ μm and vanished for a radius upper than 0.320 μm, and between the two boundaries of the radius, the size of a photonic band gap was varying like a Gaussian function with a hole radius. On the other hand, the bandwidth is maximum for $r = 0.27$ μm, it was about 117 nm. Figure 3**b** depicts the gap map of the previous triangular structure for the TM polarization. We can observe that the forbidden band extends between $a/\lambda = 0.40$ and 0.56 when the radius of air holes is varied from 0.131 to 0.320 μm. Furthermore, the results show that the largest band gap was found around telecommunications wavelength $\lambda = 1.55$ μm, which corresponds to the TM polarization and it extends from $\lambda_{min} = 1.485$ μm to $\lambda_{max} = 1.602$ μm. These results have been obtained by using the 2D PWE technique [14].

3. Two-dimensional magneto-photonic waveguide

Figure 4 shows the top view of the physical design that we analyze and simulate in this work. It is a linear and symmetric 2D magneto-photonic waveguide ($W3_A^K$), which is realized on the wafer of SiO_2/TiO_2 matrix by removing three rows of air holes in the ΓK direction. This kind of structure is called air-bridge structure which is surrounded by air (substrate and cover). The simulations are based on the known finite difference BPM of RSoft CAD [14]. This computational method is the most widely

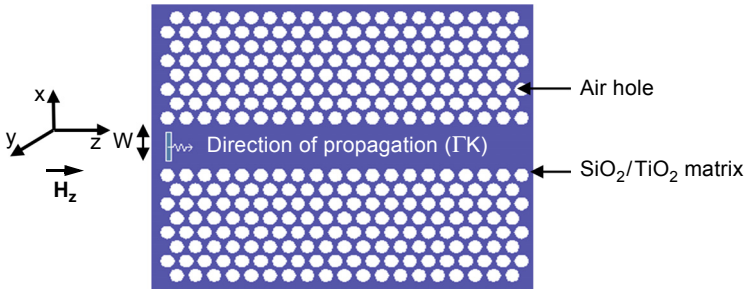

Fig. 4. Top view of a W3 waveguide in a 2D triangular lattice of air holes formed by removing three rows of holes along the ΓK direction.

used propagation technique for modeling photonic devices and photonic integrated circuits.

In this section, we will simulate the propagation in the waveguide by a Gaussian pulse excited from the light source with a normalized frequency centered at $\omega = 0.484(2c/a)$ with a frequency width of $\Delta\omega = 0.04(2c/a)$ (c is the velocity of light in free space). The 2D photonic crystals are realized on a magneto-optical matrix of silica/titania (SiO_2/TiO_2) doped with different volume fractions of cobalt ferrite nanoparticles and subjected to a magnetic field parallel to the direction of propagation.

4. Theory of the mode conversion

Magneto-optical waveguides are the basic elements for nonreciprocal integrated optics. However, the application of a magnetic field on a magneto-optical material with a direction parallel to the light beam propagation (Oz) produces off-diagonal elements in a dielectric tensor where the magnitude depends on the Faraday rotation θ_F and ellipticity ε_F [18]. Faraday rotation depends on several parameters such as the nanoparticle size [19], the particle volume fraction [20], the applied magnetic field [21] and the light wavelength [22]. Similar to the Faraday rotation effect observed in free space, a nonreciprocal effect can be achieved in a planar waveguide by the TE-TM mode conversion under a longitudinal magnetic field, and TE-TM mode coupling of a guide is obtained. In the case of such structure, the magneto-optical permittivity tensor $[\varepsilon]$ is expressed in a Cartesian coordinate system $\{x, y, z\}$ by:

$$[\varepsilon] = \begin{bmatrix} \varepsilon_1 & i\varepsilon_{xy} & 0 \\ -i\varepsilon_{xy} & \varepsilon_1 & 0 \\ 0 & 0 & \varepsilon_1 \end{bmatrix} \tag{1}$$

where ε_1 and λ are respectively the value of diagonal elements of a permittivity tensor ($\varepsilon_1 = 2.4964$) and the wavelength of work.

The off-diagonal element (ε_{xy}) of a permittivity tensor leads to a coupling between the TE and TM modes. It strongly depends on the Faraday rotation θ_F which is proportional to the concentration of magnetic nanoparticles $\Phi_{\%}$, vacuum wavelength λ and the refractive index of the magneto-optical (mo) material ($n = \sqrt{\varepsilon_1}$). The magnitude of ε_{xy} is given by the approximate relationship [23, 24]:

$$\varepsilon_{xy} = \mathrm{Im}(\varepsilon_{\mathrm{mo}}) = \frac{\theta_F \lambda \sqrt{\varepsilon_1}}{\pi} \tag{2}$$

Here, for simplicity, we will ignore the absorption and assume ε_1 and ε_{xy} to be real. If the incident mode is the transverse magnetic (TM), the conversion output $R(z)$ is defined like the intensity ratio of the mode TE at the distance z on the intensity of the mode TM at the beginning ($z = 0$) [5]:

$$R(z) = I_{\mathrm{TE}(z)} / I_{\mathrm{TM}(0)} \tag{3}$$

It can then be written as:

$$R(z) = \frac{\theta_F^2}{\theta_F^2 + (\Delta\beta/2)^2} \sin^2\left[\sqrt{\theta_F^2 + (\Delta\beta/2)^2}\, z\right] \tag{4}$$

From Eq. (4), it is clear that TE-TM mode conversion is strongly affected by the specific Faraday rotation θ_F (deg/cm) of the material forming the waveguide and by the phase mismatch between TE and TM modes $\Delta\beta$ (deg/cm) which is given by

$$\Delta\beta = \beta_{\mathrm{TE}} - \beta_{\mathrm{TM}} = (N_{\mathrm{TE}} - N_{\mathrm{TM}}) \frac{2\pi}{\lambda} \tag{5}$$

In practice, the difference between the TE and TM refractive index needs to be as low as possible for an efficient mode conversion. This later is obtained for a distance called the coupling length. When the difference of the phase $\Delta\beta$ is not zero, the conversion efficiency of the mode is limited to the value R_M which is obtained at the end of a length of coupling L_C, and it is given by the relationship [25]:

$$L_C = \frac{\pi}{\sqrt{4\theta_F^2 + (\Delta\beta)^2}} \tag{6}$$

The maximum rate of mode conversion induced by a Faraday rotation effect can be expressed as:

$$R_M = \frac{\theta_F^2}{\theta_F^2 + (\Delta\beta/2)^2} \tag{7}$$

5. The effect of volume fraction on the mode conversion

The analysis performed in this work has been concentrated on the TM polarization, for which the 2D photonic crystal exhibits a band gap between $\lambda = 1485$ nm and 1602 nm. In Figure 5**a**, we report the *E*-field distribution inside the guide and the power flow through the waveguide for the TM mode. It is clear that, for an isotropic planar waveguide and hence for a zero magnetization ($\varepsilon_{xy} = 0$), there is no coupling between TE and TM modes. On the contrary, once the volume fraction of cobalt ferrite increases inside 2D magneto-photonic waveguide, so the magnitude of ε_{xy} increases, and the modes start to couple between them. Figure 5**b** shows the *E*-field distribution and the mode conversion obtained with a BPM in the case of a sol-gel SiO_2/TiO_2 matrix of thickness $h = 2.4$ µm and doped with 18% of $CoFe_2O_4$ nanoparticles. The magnitude

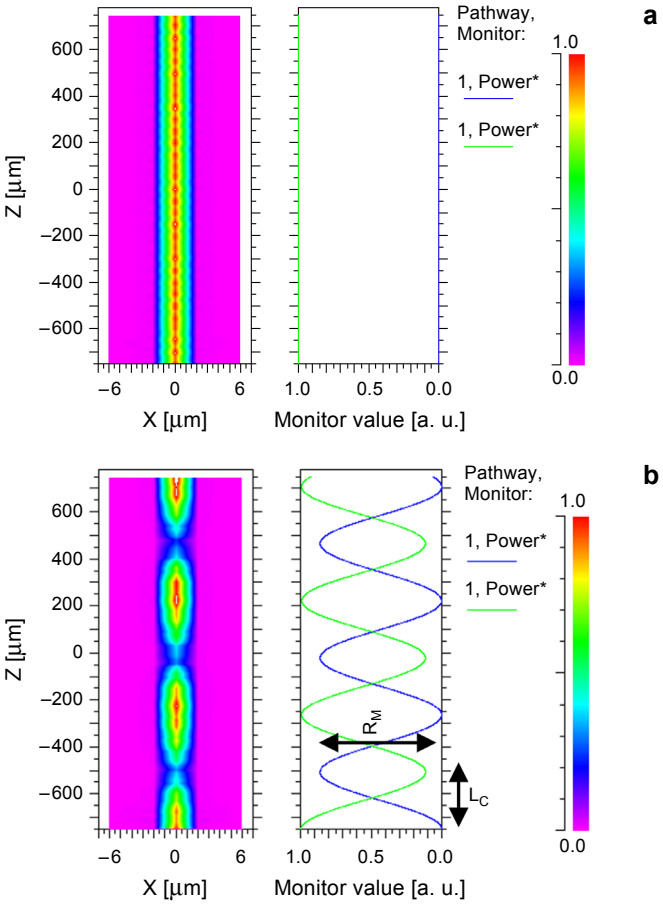

Fig. 5. Mode conversion in isotropic planar waveguide (**a**), mode conversion in 2D magneto-photonic waveguide doped with 18% of $CoFe_2O_4$ nanoparticles (**b**).

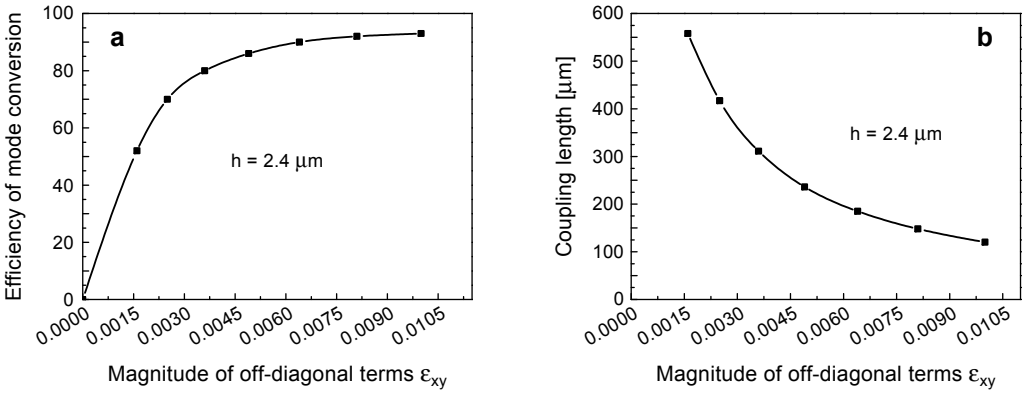

Fig. 6. The influence of the off-diagonal elements ε_{xy} for a sol-gel silica/titania matrix of thickness $h = 2.4$ μm: on the conversion output R_M (**a**), and on the coupling length L_C (**b**).

of magneto-optical term ε_{xy} is calculated using the corresponding value of θ_F, derived from [25], and Eq. (2), and it is found to be 0.004761.

Figures 6**a** and 6**b** report, respectively, the influence of the off-diagonal term ε_{xy} on the conversion output R_M and the coupling length L_C for a slab of thickness $h = 2.4$ μm. We observe that, if the value of the off-diagonal term ε_{xy} increases, the coupling length L_C decreases and the maximal conversion R_M increases, thus the time necessary to obtain the coupling decreases. Thus, the efficiency of mode conversion R_M when the magneto-optical layer is doped with a weak concentration of magnetic nanoparticles $\varepsilon_{xy} = 0.0016$ is 52% and reached 95% for high concentration $\varepsilon_{xy} = 0.0104$. The coupling length is about 558 μm for $\varepsilon_{xy} = 0.0016$ and decreases to 115 μm for $\varepsilon_{xy} = 0.0104$.

6. The effect of slab height on the conversion output

In the following section, we consider the magneto-photonic structure described above and doped with a high volume fraction of cobalt ferrite (39%) [25]. The Faraday rotation is about 8034 deg/cm, consequently, the off-diagonal term of a permittivity tensor has the value $\varepsilon_{xy} = 0.0104$, which corresponds to a strong coupling between the TE/TM modes. Now, the light propagation inside the planar magneto-photonic waveguide is simulated as a function of various slab thickness to obtain the maximum mode conversion. The 3D BPM was employed in order to obtain different results which are depicted in Fig. 7.

Figure 7 represents the variation of the conversion output and the coupling length according to the thickness of slab height h, for this concentration. It is observed that the conversion output increases proportionally to the increase in slab thickness h when the thickness of SiO_2/TiO_2 film increases between 1.6 and 2.6 μm. The value of con-

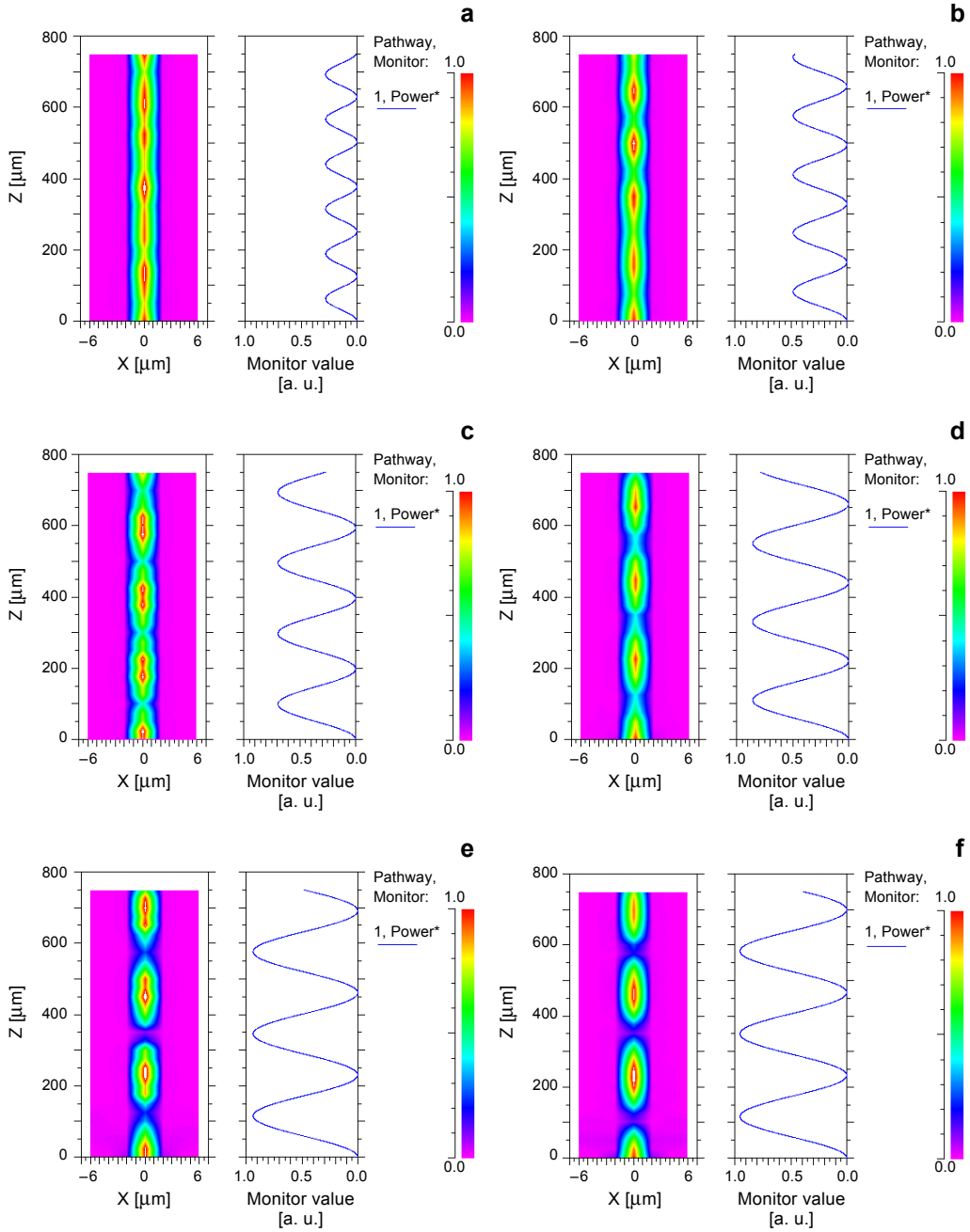

Fig. 7. The effect of thickness on the mode conversion in a 2D magneto-photonic waveguide structure formed by a triangular lattice of air holes in SiO_2/TiO_2 matrix doped with 39% for: $h = 1.6$ µm (**a**), $h = 1.8$ µm (**b**), $h = 2.0$ µm (**c**), $h = 2.2$ µm (**d**), $h = 2.4$ µm (**e**), and $h = 2.6$ µm (**f**).

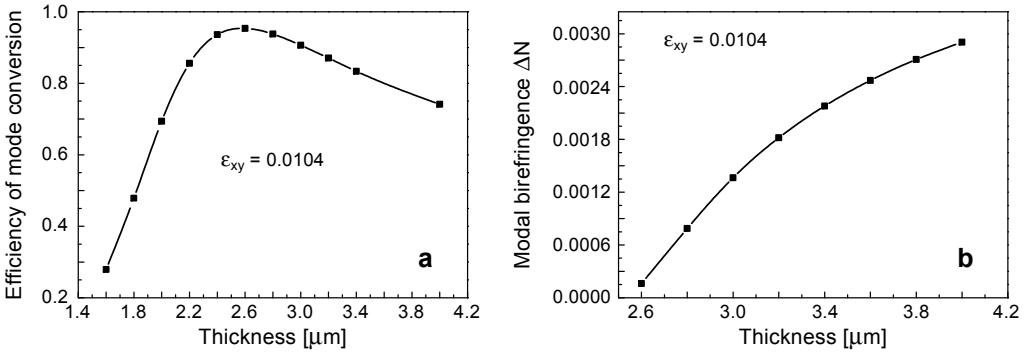

Fig. 8. The influence of the film thickness h on the mode conversion output (**a**) and on the phase mismatch (**b**) for a sol-gel matrix doped with 39% of $CoFe_2O_4$.

version output is 27.90% for $h = 1.6$ μm and it reaches the value of 95.34% for $h = 2.6$ μm. Beyond the value of 2.6 μm, the output conversion decreases and reaches 74.10% for $h = 4.0$ μm as it is shown in Fig. 8**a**.

7. The effect of slab height on the modal birefringence

The conception of a magneto-optical isolator that has an interesting nonreciprocal effect needs the maximization of R_M. To achieve this goal, the amplitude of the specific Faraday rotation θ_F (deg/cm) must be as high as possible, while the phase mismatch between TE and TM modes $\Delta\beta$ (deg/cm) must be as low as possible. This later is directly linked to the geometrical modal birefringence ΔN_m for the mode number m by the following relationship [26]:

$$\Delta\beta_m = \Delta N_m \frac{2\pi}{\lambda} \tag{8}$$

As it is shown in Fig. 8**b**, we have calculated the influence of the film thickness h on the modal birefringence (ΔN, $m = 0$) for the mode TM_0. The obtained results show clearly that, if the slab thickness h increases, the modal birefringence decreases. Thus, for a sol-gel SiO_2/TiO_2 matrix of thickness $h = 4.0$ μm the modal birefringence between the fundamental TE_0 and TM_0 modes was equal to $\Delta N_0 = 29.05 \times 10^{-4}$, and it reaches 1.6×10^{-4} for a slab thickness $h = 2.6$ μm.

8. Conclusion

This paper describes a theoretical study of a 2D magneto-photonic waveguide formed by a triangular lattice of circular air holes embedded into silica/titania matrix. It is prepared via a sol-gel process and doped with ferrite of cobalt nanoparticles. This new magneto-optical material is fully compatible with classical substrates. Firstly, using

a 2D PWE method we have studied and analyzed the band diagrams and the gap maps in 2D photonic crystals in order to determine the photonic band gaps.

Afterwards, an analysis of the mode conversion in a 2D magneto-photonic crystal waveguide has been presented, using the BPM, in order to provide a theoretical prediction of physical and geometrical parameters that lead to an efficient mode conversion and the enhancement of Faraday rotation. The obtained results show that the volume fraction of magnetic nanoparticles and the thickness of the film have a great influence on the mode conversion output and coupling length. We also found, for such structure, that the conversion output reaches 95% and the coupling length is lowered to 115 μm when the magnetic nanoparticles concentration increases to 39%.

Finally, the calculation of the modal birefringence between the fundamental TE and TM modes, as a function of slab thickness, show clearly that a decrease in the modal birefringence occurs when the slab thickness is decreased. Consequently, the conversion output is strongly affected by the film thickness.

A future work consists in studying the influence of the absorption coefficient on the TE/TM mode conversion in 2D magneto-photonic crystal waveguides devices.

References

[1] BAHLMANN N., LOHMEYER M., ZHUROMSKYY Q., DÖTSCH H., HERTEL P., *Nonreciprocal coupled waveguides for integrated optical isolators and circulators for TM-modes*, Optics Communications **161**(4–6), 1999, pp. 330–337.

[2] BAHLMANN N., LOHMEYER M., DÖTSCH H., HERTEL P., *Integrated magneto-optic Mach–Zehnder interferometer isolator for TE modes*, Electronics Letters **34**(22), 1998, pp. 2122–2123.

[3] XIAOYUN GUO, ZAMAN T., RAM R.J., *Magneto-optical semiconductor waveguides for integrated isolators*, Proceedings of SPIE **5729**, 2005, pp. 152–159.

[4] LANO G.E., PINYAN C., *Optical isolators direct light the right way: fiberoptic components handbook*, Laser Focus World **31**(7), 1995, pp. 125–127.

[5] LOHMEYER M., BAHLMANN N., ZHUROMSKYY O., DÖTSCH H., HERTEL P., *Phase-matched rectangular magnetooptic waveguides for applications in integrated optics isolators: numerical assessment*, Optics Communications **158**(1–6), 1998, pp. 189–200.

[6] HUANG M., XU Z.-C., *Wavelength and temperature characteristics of BiYbIG film/YIG crystal composite structure for magneto-optical applications*, Applied Physics A **81**(1), 2005, pp. 193–196.

[7] HUTCHINGS D.C., *Prospects for the implementation of magneto-optic elements in optoelectronic integrated circuits: a personal perspective*, Journal of Physics D: Applied Physics **36**(18), 2003, pp. 2222–2230.

[8] HOCINI A., BOUMAZA T., BOUCHEMAT M., ROYER F., JAMON D., ROSSEAU J.J., *Birefringence in magneto -optical rib waveguides made by SiO_2/TiO_2 doped with γ-Fe_2O_4*, Microelectronics Journal **39**(1), 2008, pp. 99–102.

[9] ROYER F., JAMON D., BROQUIN J.-E., AMATA H., KEKESI R., NEVEU S., BLANC-MIGNON M.-F., GHIBAUDO E., *Fully compatible magneto-optical sol-gel material with glass waveguides technologies: application to mode converters*, Proceedings of SPIE **7941**, 2011, article 794106.

[10] SHOJI Y., MIZUMOTO T., YOKOI H., HSIEH I.-W., OSGOOD R.M., JR, *Magneto-optical isolator with silicon waveguides fabricated by direct bonding*, Applied Physics Letters **92**(7), 2008, article 071117.

[11] JOUDRIER A.-L., COUCHAUD M., MORICEAU H., BROQUIN J.-E., FERRAND B., DESCHANVRES J.-L., *Direct bonding conditions of ferrite garnet layer on ion-exchanged glass waveguides*, Physica Status Solidi (A) **205**(10), 2008, pp. 2313–2316.

[12] CHOUEIKANI F., ROYER F., JAMON D., SIBLINI A., ROUSSEAU J.J., NEVEU S., CHARARA J., *Magneto-optical waveguides made of cobalt ferrite nanoparticles embedded in silica/zirconia organic-inorganic matrix*, Applied Physics Letters **94**(5), 2009, article 051113.
[13] KAHLOUCHE A., HOCINI A., KHEDROUCHE D., *Band-gap properties of 2D photonic crystal made by silica matrix doped with magnetic nanoparticles*, Journal of Computational Electronics **13**(2), 2014, pp. 490–495.
[14] Photonic Component Design Suite, BandSOLVE, BeamPROP from Rsoft Inc., www.rsoftdesign.com
[15] MATTHEWS A., WANG X.-H., KIVSHAR Y., GU M., *Band-gap properties of two-dimensional low-index photonic crystals*, Applied Physics B **81**(2–3), 2005, pp. 189–192.
[16] DYOGTYEV A.V., SUKHOIVANOV I.A., DE LA RUE R.M., *Photonic band-gap maps for different two dimensionally periodic photonic crystal structures*, Journal of Applied Physics **107**(1), 2010, article 013108.
[17] AMATA H., ROYER F., CHOUEIKANI F., JAMON D., BROQUIN J.-E., PLENET J.C., ROUSSEAU J.J., *Magnetic nanoparticles-doped silica layer reported on ion-exchanged glass waveguide: towards integrated magneto-optical devices*, Proceedings of SPIE **7719**, 2010, article 77191G.
[18] WITTEKOEK S., POPMA T.J.A., ROBERTSON J.M., BONGERS P.F., *Magneto-optic spectra and the dielectric tensor elements of bismuth substituted iron garnets at photon energies between 2.2–5.2 eV*, Physical Review B **12**(7), 1975, p. 2777.
[19] ROYER F., JAMON D., ROUSSEAU J.J., CABUIL V., ZINS D., ROUX H., BOVIER C., *Experimental investigation on γ-Fe_2O_3 nanoparticles Faraday rotation: particles size dependence*, European Physical Journal Applied Physics **22**(2), 2003, pp. 83–87.
[20] KAHLOUCHE A., HOCINI A., KHEDROUCHE D., *Mode conversion in 2D magneto photonic crystals made of SiO_2/ZrO_2 matrix doped with magnetic nanoparticles*, Acta Physica Polonica A **127**(4), 2015, pp. 1208–1210.
[21] DAVIES H.W., LLEWELLYN J.P., *Magneto-optic effects in ferrofluids*, Journal of Physics D: Applied Physics **13**(12), 1980, pp. 2327–2337.
[22] DONATINI F., JAMON D., MONIN J., NEVEU S., *Experimental investigation of longitudinal magneto-optic effects in four ferrite ferrofluids in visible-near infrared spectrum*, IEEE Transactions on Magnetics **35**(5), 1999, pp. 4311–4317.
[23] BOURAS M., HOCINI A., *Mode conversion in magneto-optic rib waveguide made by silica matrix doped with magnetic nanoparticles*, Optics Communications **363**, 2016, pp. 138–144.
[24] HOCINI A., BOUMAZA T., BOUCHEMAT M., CHOUEIKANI F., ROYER F., ROUSSEAU J.J., *Modeling and analysis of birefringence in magneto-optical thin film made by SiO_2/ZrO_2 doped with ferrite of cobalt*, Applied Physics B **99**(3), 2010, pp. 553–558.
[25] KEKESI R., ROYER F., JAMONA D., BLANC-MIGNON M.F., ABOU-DIWAN E., CHATELON J.P., NEVEU S., TOMBACZ E., *3D magneto-photonic crystal made with cobalt ferrite nanoparticles silica composite structured as inverse opal*, Optical Materials Express **3**(7), 2013, pp. 935–947.
[26] HOCINI A., BOUCHELAGHEM A., SAIGAA D., BOURAS M., BOUMAZA T., BOUCHEMAT M., *Birefringence properties of magneto-optic rib waveguide as a function of refractive index*, Journal of Computational Electronics **12**(1), 2013, pp. 50–55.

Received December 23, 2015
in revised form March 15, 2016